

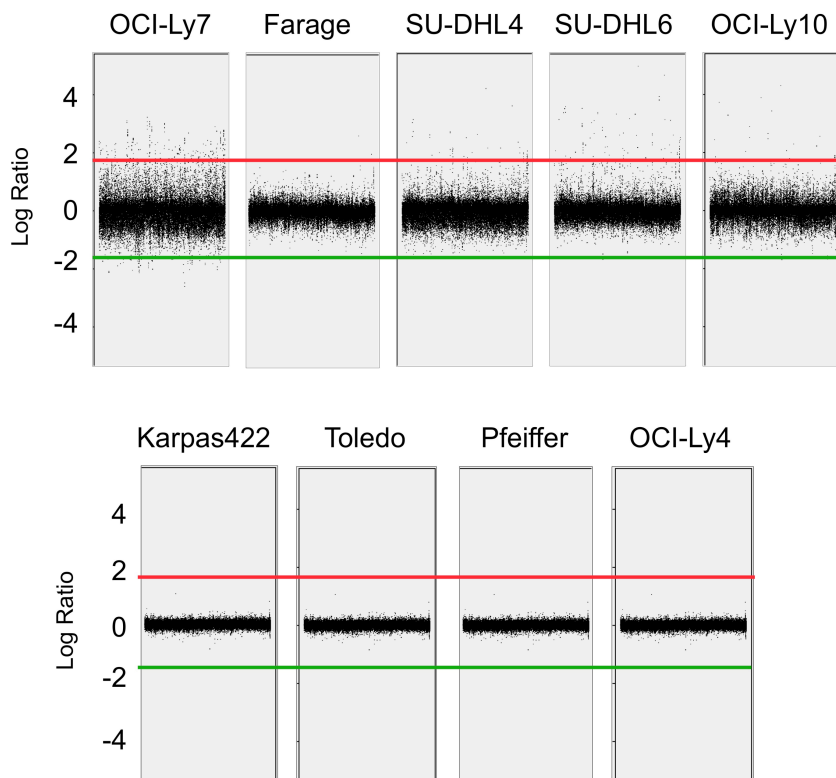
BCL6 repression of *EP300* provides a basis for rational combinatorial therapy in human diffuse large B cell lymphoma cells

Leandro C. Cerchietti^{1,2}, Katerina Hatzl^{1,2}, Eloisi Caldas-Lopes³, Shao Ning Yang^{1,2}, Maria E. Figueroa^{1,2}, Ryan D. Morin⁴, Martin Hirst⁴, Lourdes Mendez¹, Rita Shaknovich^{1,2}, Philip A. Cole⁵, Kapil Bhalla⁶, Randy D. Gascoyne⁷, Marco Marra⁴, Gabriela Chiosis³, Ari Melnick^{1,2}.

1. Hematology and Oncology Division. Weill Cornell Medical College. New York, NY.
2. Department of Pharmacology. Weill Cornell Medical College. Cornell University. New York, NY.
3. Department of Molecular Pharmacology and Chemistry, Sloan-Kettering Institute, New York, NY.
4. Genome Sciences Centre, British Columbia Cancer Agency, Vancouver, BC.
5. Department of Pharmacology and Molecular Sciences. Johns Hopkins University School of Medicine. Baltimore, MD.
6. The University of Kansas Cancer Center, Kansas University Medical Center, Kansas City, KS.
7. Centre for Lymphoid Cancers and the Departments of Pathology and Experimental Therapeutics, British Columbia Cancer Agency, British Columbia Cancer Research Centre, Vancouver, BC.

Figure S1

A



B

UP-REGULATED		DOWN-REGULATED	
ANTRX1	HN1	MUC11	ABCD1
BC000845	HSPA6	MUC3	C13ORF18
C16ORF72	IL1RL1	MUC4	CYTH4
CD274	KIR2DL3	OR2M5	NRLC3
CD55	KRTAP21-1	OR2M7	NUP210
CRLF2	LOC284861	OR4F16	OPRL1
CSAG2	LOC349196	OR4F29	SIPA1L3
CYSLTR2	LOC65122	OR4K2	SLC16A13
DNAJA4	MT-ATP6	PSG1	
DUB3	MT-CYB	REXO1L1	
DUSP5	MT-ND2	S100A7	
ETV3	MT-ND3	SEMG1	
FOSB	MT-ND6	SPRR2A	
GAGE1		SPRYD5	
GAGE3		TRIM51	
GAGE5			

Figure S1. A core RI-BPI response signature in BCL6 dependent DLBCL cells. **A:** Dot-plots of log-ratio intensity (Y-axis) vs. probe (X-axis) in a panel of five BCL6- dependent DLBCL cell lines (OCI-Ly7, Farage, SU-DHL4, SU-DHL6, and OCI-Ly10) and four BCL6-independent DLBCL cell lines (Karpas422, Toledo, Pfeiffer and OCI-Ly4). Log-ratios were obtained by comparison of the genes mobilized in RI-BPI 10 μ M treated cells (Cy3 channel) over the genes mobilized in CP 10 μ M treated cells (Cy5 channel) in each cell line. Cells were exposed to treatments for 24 h. Experiments were carried out in duplicates. Up- and down-regulated probes were defined by a cut-off of log-ratio ≥ 1.8 (shown by the red and green lines respectively). The up- and down-regulated probes common to all RI-BPI-responsive cell lines were considered the core gene expression signature. **B:** The list of genes in the RI-BPI core signature, which was used to query the connectivity map. Previously known BCL6-target genes are shown in bold.

Figure S2

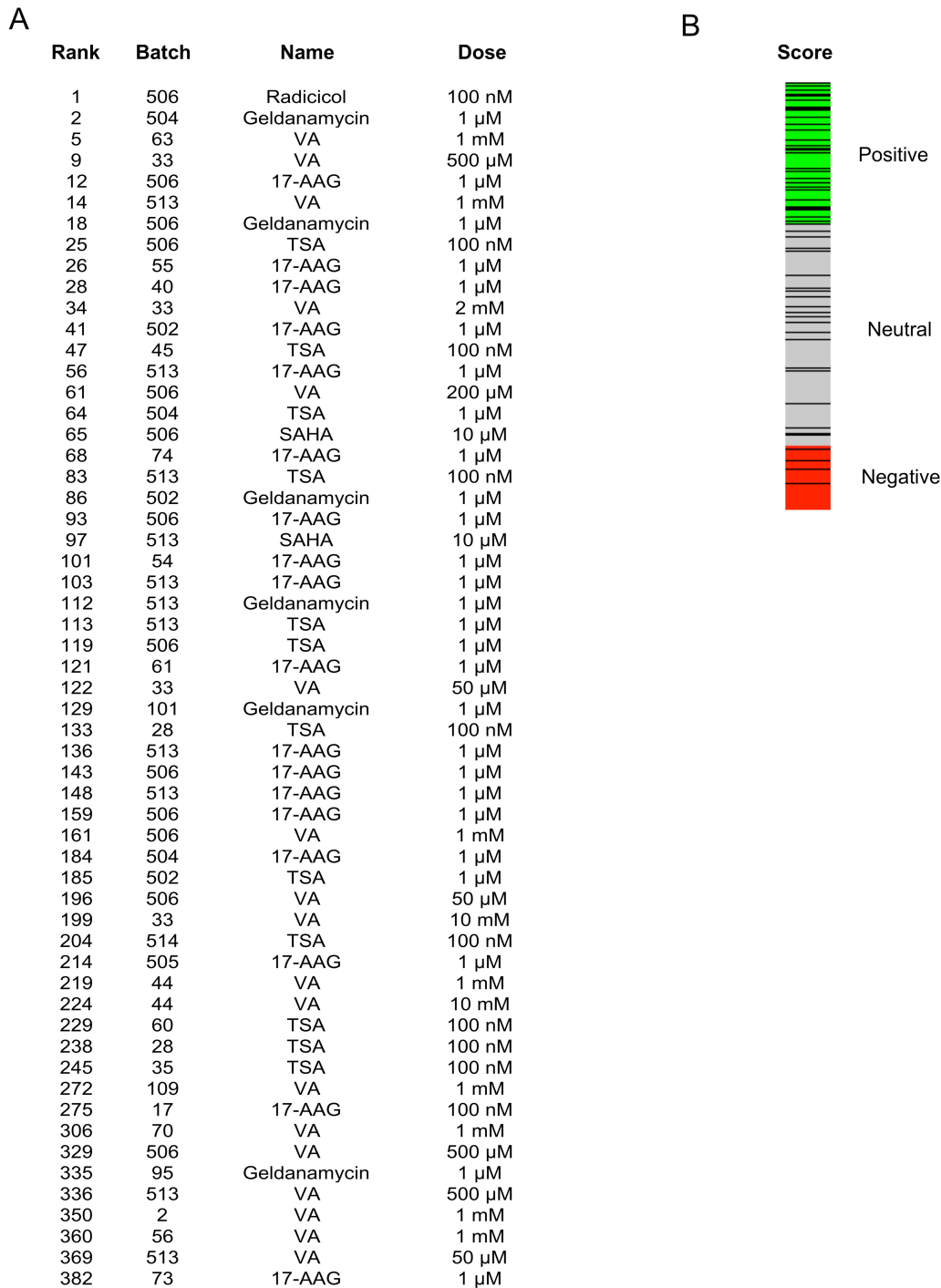


Figure S2. Connectivity map analysis of RI-BPI reveals potential functional relationship with Hsp90 inhibitors and HDI. A: Connectivity-map query result for the RI-BPI genomic signature. The list shows ranking of Hsp90 inhibitors (Radicicol, Geldanamycin, 17-AAG) and HDAC inhibitors (TSA, SAHA and VA), with the associated batch and dose used to generate the database. **B:** Connectivity score (positive, negative and neutral) for the RI-BPI genomic signature and the Hsp90 inhibitors and HDI.

Figure S3

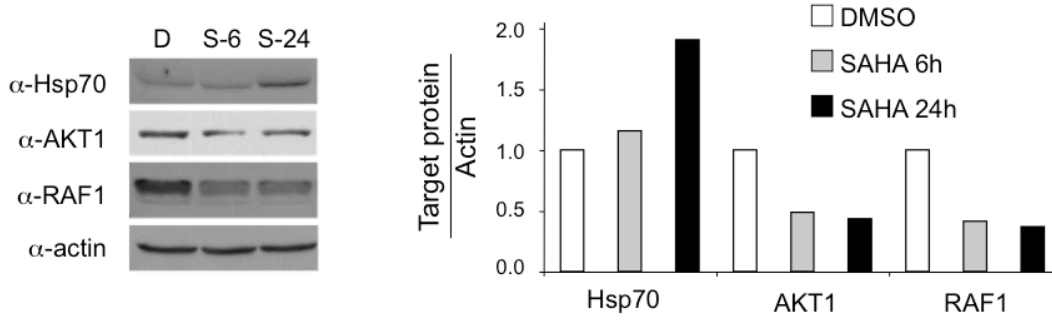


Figure S3. SAHA induces degradation of Hsp90 client proteins and induction of Hsp70. Immunoblotting was performed for Hsp70, AKT1, RAF1 and actin (as control) in cell extracts of OCI-Ly7 cells treated with SAHA 1 μ M for 6 and 24 h. Densitometry analysis is shown on the right.

Figure S4

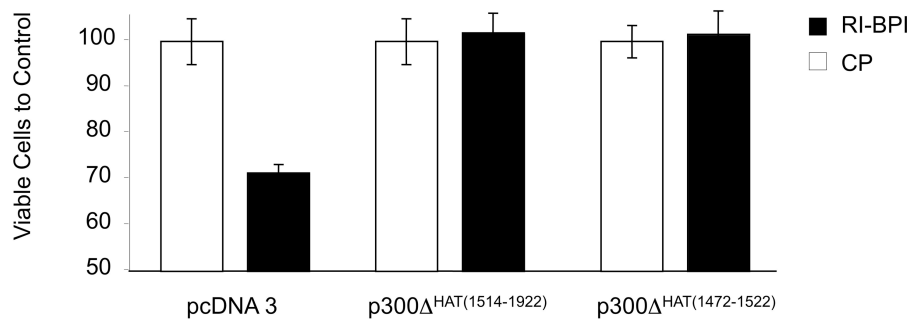


Figure S4. RI-BPI-induced cell death is rescued by dominant negative p300 Δ KAT. SU-DHL6 cells were transfected with two different p300-KAT dominant-negative constructs (P300 Δ ^{KAT(1514-1922)} and p300 Δ ^{KAT(1472-1522)}) or control (pcDNA3) followed by treatment with RI-BPI 10 μ M (black bars) or CP (white bars). After 48 h the viability was determined using a metabolic assay. Experiments were done in duplicates. Bars represent S.E.M. for duplicates.

Figure S5

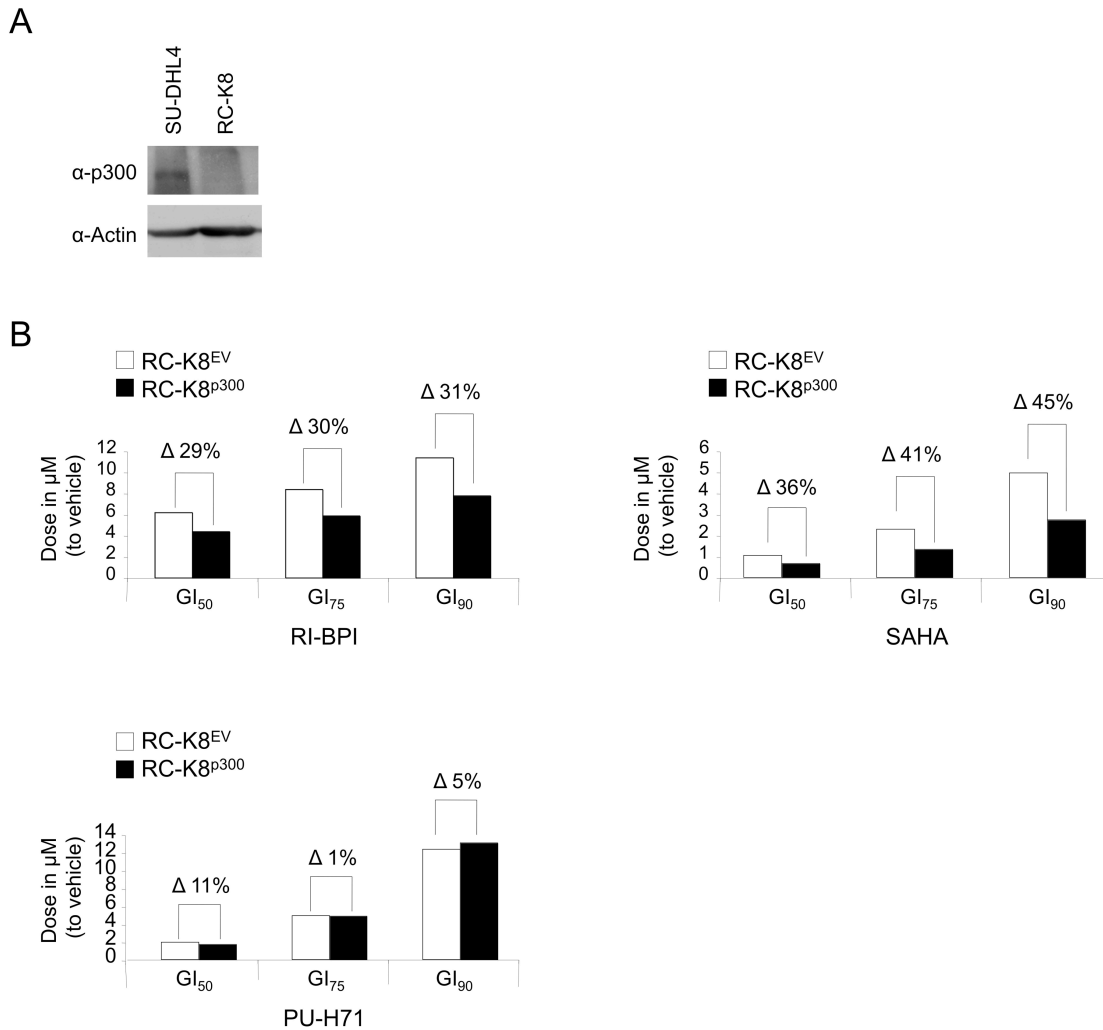


Figure S5. Expression of wild type p300 expression enhances response to RI-BPI and SAHA in *EP300* null DLBCL cells. **A:** Immunoblot for p300 (N-15) and actin (as control) in the SU-DHL4 and RC-K8 DLBCL cell lines. **B:** Drug doses (Y-axis) correspondent to the Growth Inhibition (GI)₅₀, GI₇₅ and GI₉₀ of RI-BPI, SAHA and PU-H71 in RC-K8 cells transfected with a p300 plasmid (RC-K8^{p300}, Black bars) or its correspondent empty vector (RC-K8^{EV}, white bars). The difference in the dose required to achieve the respective growth inhibition concentrations between RC-K8^{EV} and RC-K8^{p300} are indicated as percentage.

Figure S6

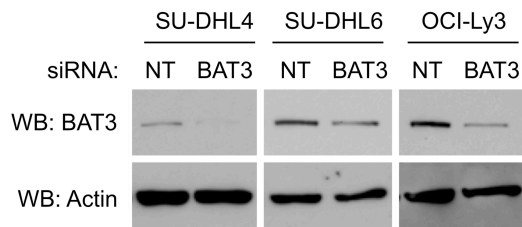


Figure S6. Confirmation of the efficacy of *BAT3* siRNA. SU-DHL4, SU-DHL6 and OCI-Ly3 cells were electroporated with siRNA targeting *BAT3* or with non-targeting siRNA (NT). Protein abundance was determined by immunoblot. Actin was used as loading control.

Figure S7

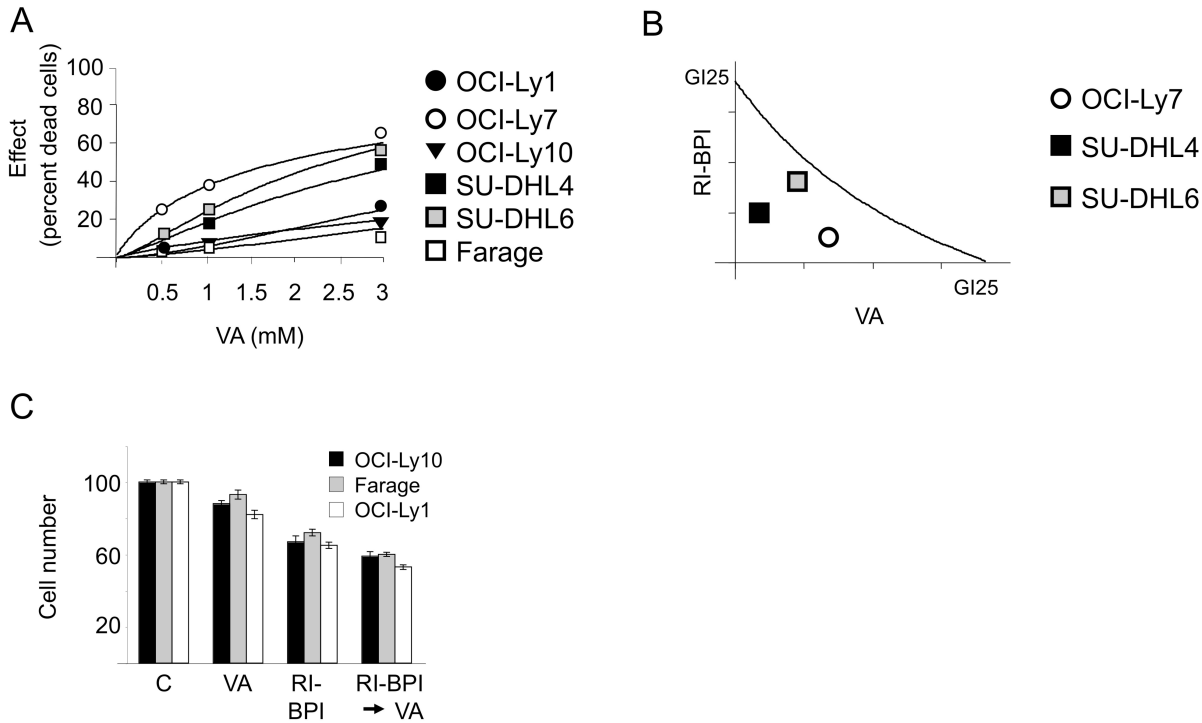


Figure S7. RI-BPI exhibits additive to synergistic effects with the HDAC inhibitor valproic acid (VA). **A:** A panel of six BCL6-dependent DLBCL cell lines (OCI-Ly7, SU-DHL6, OCI-Ly1, Farage, SU-DHL4 and OCI-Ly10) was exposed in triplicate to five concentrations of VA (from 0.125 to 3 mM) or vehicle control (water) for 48 h and analyzed for cell viability. Dose-effect (percent dead cells) curves were plotted. The X-axis shows the dose of VA. The Y-axis shows the fractional effect of VA as compared to control on cell viability. **B:** The cell lines for which a VA GI₂₅ was obtained (OCI-Ly7, SUDHL-4 and SU-DHL6), were treated with five concentrations of VA, RI-BPI and the combination in a constant ratio (concurrent schedule). A conservative GI₂₅ isobologram for the combination of VA with RI-BPI was plotted for each particular cell line. The dose values for each GI₂₅ for each cell line are shown in **Table S1**. **C:** For the cell lines that were resistant to VA (i.e.: the GI₂₅ was higher than the upper dose limit), a potentiation effect with RI-BPI was calculated. OCI-Ly10, OCI-Ly1 and Farage cells were treated with 10 μM RI-BPI, 1 mM VA or the combination for 48 h (sequential schedule BPI→drug). Cell viability was determined and compared to control treated cells (water).

Figure S8

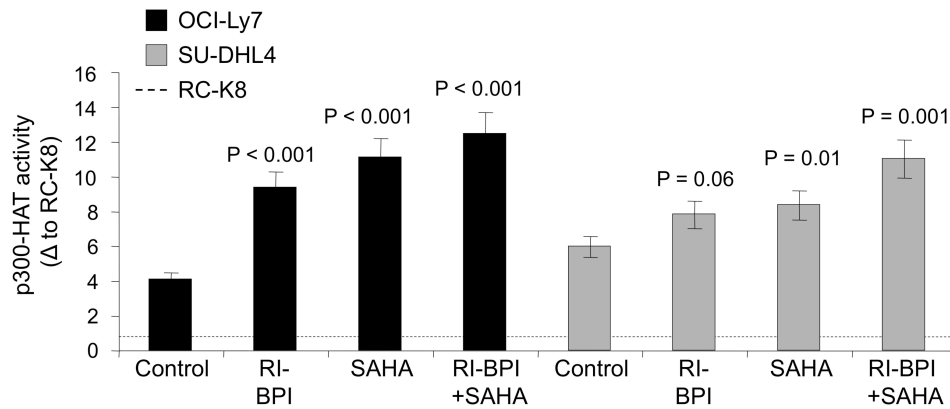


Figure S8. The combination of RI-BPI and SAHA increases p300 KAT activity to a greater level than either drug alone. P300-HAT activity was measured in OCI-Ly7 (black bars) and SU-DHL4 (grey bars) cells before (control) and after treatment with 10 μ M RI-BPI, 1 μ M SAHA or SAHA + BPI for 24 h normalized to the P300-HAT activity in RC-K8 cells (dotted line). The HAT-activity associated with p300 was determined by p300 IP vs. IgG followed by incubation of the immunoprecipitates with specific HAT substrates and cofactors. The resulting acetylated product was measured by spectrophotometry (OD_{440nm}). Results expressed in fold induction vs. control.

Figure S9

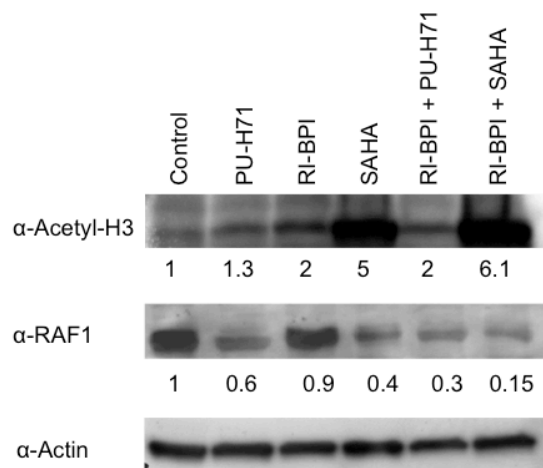


Figure S9. Effect of the combined drug treatment on the abundance of RAF1 and acetyl-H3. Immunoblotting for acetyl-H3, RAF1 and actin (as control) for OCI-Ly7 cells treated with 1 μ M PU-H71, 10 μ M BPI, 1 μ M SAHA and the combination of PU-H71 + BPI and SAHA + BPI for 24 h. The numeric values represent the ratio between the densitometry for acetyl-H3 and RAF1 vs. actin for each lane.

Figure S10

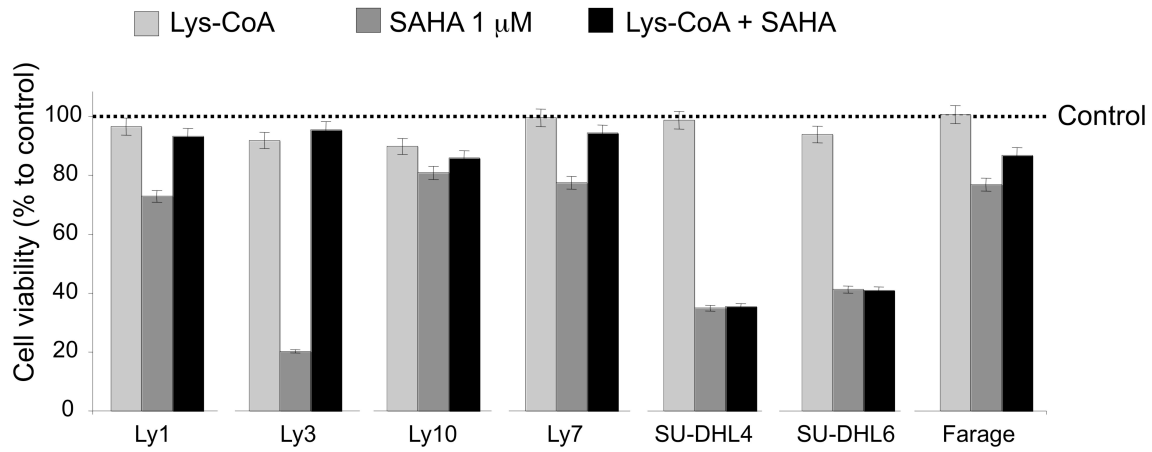


Figure S10. SAHA-induced cell death is partially rescued by p300 inhibition. A panel of seven BCL6-dependent DLBCL cell lines (OCI-Ly7, SU-DHL6, OCI-Ly1, Farage, OCI-Ly3, SU-DHL4 and OCI-Ly10) was exposed in triplicate to 1 μM SAHA (dark grey bars), the p300-HAT inhibitor Lys-CoA-TAT (light grey bars) and the combination of both (black bars) for 48 h. Cell viability (as percent to control) is shown on the Y-Axis.

Figure S11

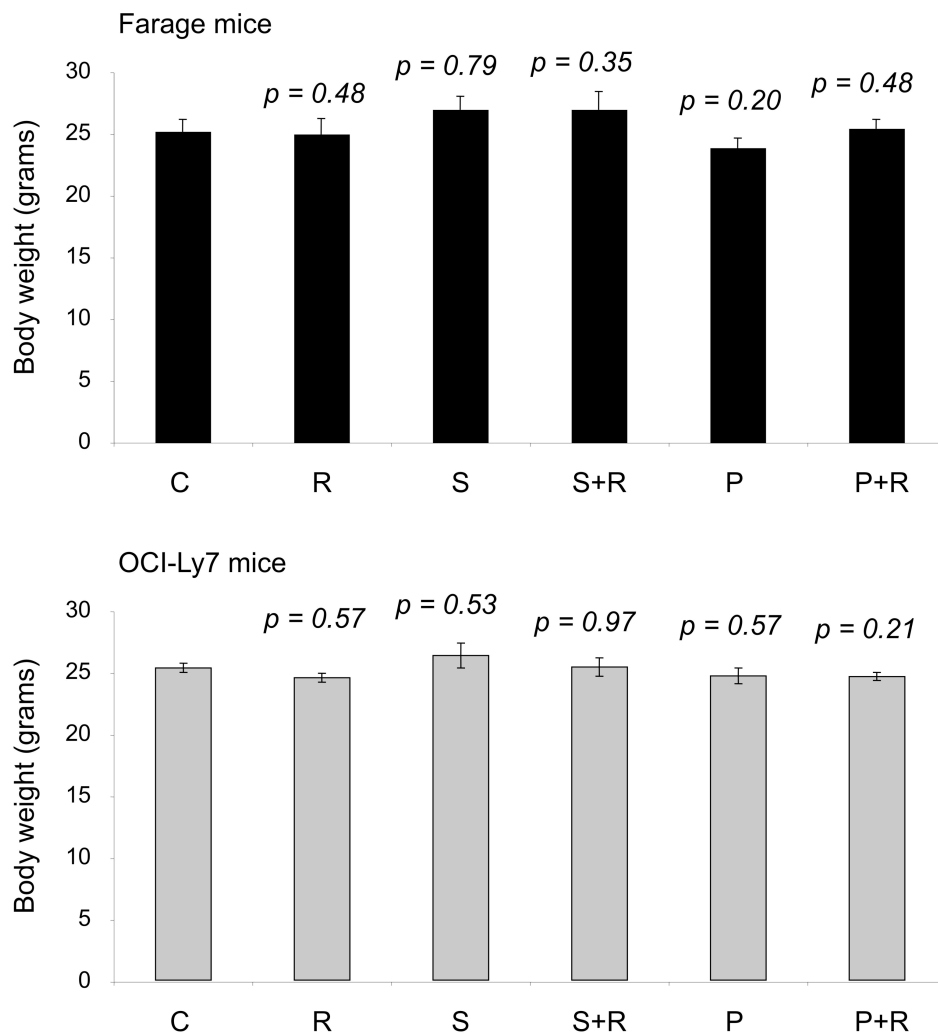


Figure S11. Body weight of mice after treatment with anti-lymphoma drugs. The columns represent the average of the body weight (with the SE) for the mice bearing Farage (top) and OCI-Ly7 (bottom) xenografts treated with vehicle control (C), RI-BPI (R), SAHA (S), PU-H71 (P), SAHA + RI-BPI (S+R) and PU-H71 + RI-BPI (P+R). The body weight was adjusted to tumor weight. The p values correspond to the two-tailed T-test comparison with the vehicle control mice.

Figure S12

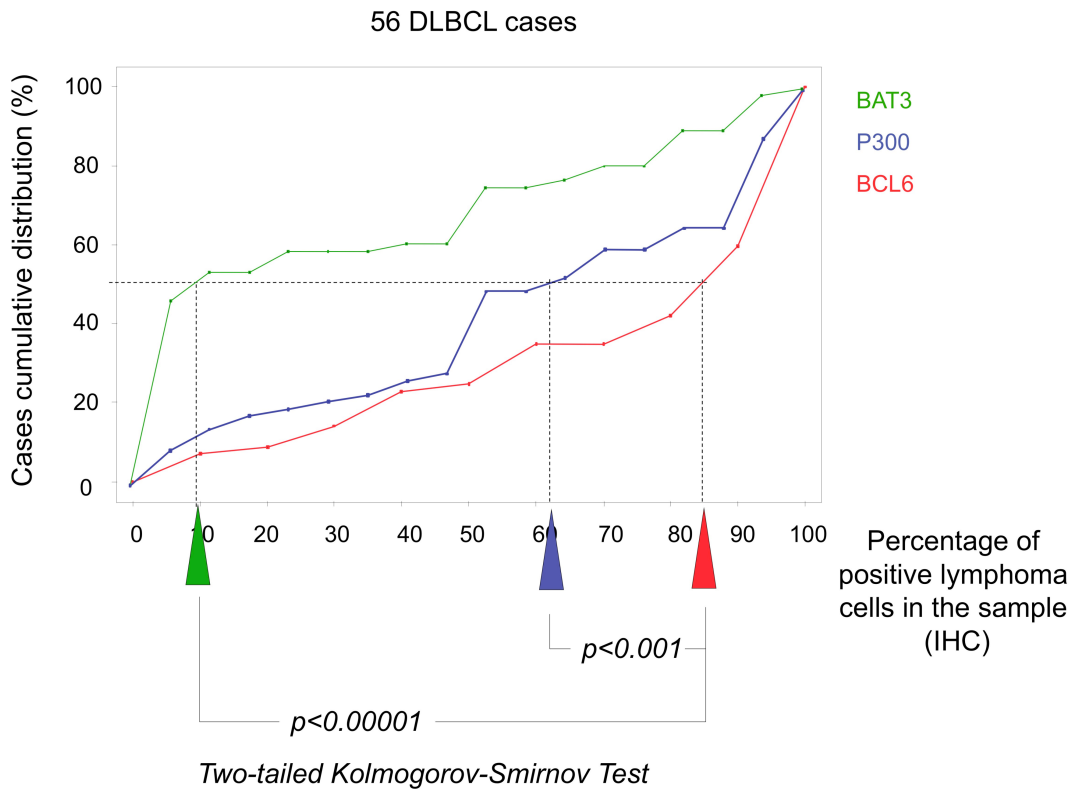


Figure S12. BCL6, p300 and BAT3 expression in DLBCL cases. The presence of BCL6, p300 and BAT3 was determined by immunohistochemistry in a TMA including 57 DLBCL cases. The percentage of positive lymphoma cells for each protein per sample (X-axis) was plotted against the cumulative distribution of cases (Y-axis). The arrows indicate the median percentage of positive cells corresponding to 50% of the cases (BAT3: 38%, P300: 62%, and BCL6: 85%). The closer a curve is to upper left corner, the lower the number of positive cells. The closer a curve is to the lower right corner, the higher the number of positive cells.

Table S1

	GI₅₀ RI-BPI (μM)	GI₅₀ PUH71 (μM)	GI₅₀ 17-DMAG (μM)
Farage	7.9 (5.6-11.2)	0.72 (0.68-0.77)	0.49 (0.30-0.81)
OCI-Ly1	13.3 (8.5-20)	0.92 (0.27-1.80)	0.68 (0.35-1.34)
OCI-Ly7	16.9 (12.6-22)	0.31 (0.18-0.55)	0.33 (0.13-0.92)
OCI-Ly10	13 (8-21)	3.53 (1.11-5.61)	1.77 (1.47-2.14)
SU-DHL6	7.1 (4.6-11)	0.35 (0.22-0.57)	0.32 (0.13-0.83)
SU-DHL4	4.3 (3.5-5.4)	3.29 (2.39-7.69)	0.64 (0.60-0.67)
OCI-Ly3	19 (18-21)	1.37 (0.85-2.58)	4.56 (0.83-8.22)

	GI₅₀ SAHA (μM)	GI₅₀ TSA (nM)	GI₂₅ VA (mM)
Farage	1.68 (1.31-2.16)	110.5 (91-133)	>3
OCI-Ly1	2.05 (1.78-2.3)	207.3 (178-240)	>3
OCI-Ly7	0.75 (0.37-1.52)	71 (33-150)	0.35 (0.27-0.46)
OCI-Ly10	>10	1695 (1050-2735)*	>3
SU-DHL6	1.4 (1.23-1.6)	72 (57-91)	0.72 (0.68-0.76)
SU-DHL4	4.28 (3.58-5.13)	1010 (794-1283)*	1.5 (1.1-1.9)
OCI-Ly3	0.73 (0.35-1.49)	54.4 (34.1-86.8)	NA

**Calculated, NA: not available*

Table S1. GI₅₀ or GI₂₅ concentrations of RI-BPI, PU-H71, 17-DMAG, SAHA, TSA and VA obtained in the seven DLBCL cell lines used in the experiments. Values higher than the upper dose used in the experiments appear as calculated.

